Quantum Electronics **48** (4) 366–371 (2018)

https://doi.org/10.1070/QEL16634

Similarity parameter for the process of mid-IR light bullet formation

E.D. Zaloznaya, V.O.Kompanets, A.E. Dormidonov, S.V. Chekalin, V.P. Kandidov

Abstract. **We study the influence of the ratio of diffraction and dispersion lengths of a femtosecond mid-IR wave packet on the filamentation threshold power and the light bullet (LB) formation upon nonlinear optical interaction with solid-state dielectrics under the conditions of anomalous group velocity dispersion. It is found that the ratio of the threshold power of filamentation and LB formation to the critical power of stationary self-focusing is independent of the radiation wavelength and the medium characteristics and is determined by the similarity parameter, equal to the ratio of the diffraction length to the dispersion one. With an increase in the similarity parameter, the threshold power of filamentation and light bullet formation increases.**

Keywords: *light bullets, filamentation, wave packet, similarity parameter, threshold power, group velocity dispersion.*

1. Introduction

The light bullet (LB) formation phenomenon in a femtosecond filament attracts the attention of researchers by the possibility of generating extremely compressed wave packets (WPs) in a bulk medium without any guiding structures. The notion of a LB was introduced in Ref. [1], where the equation for a slowly varying WP envelope in the aberration-free approximation [2] and the second-order approximation of the dispersion theory was considered for a cubic nonlinear medium. LBs with a high degree of light field localisation in space and time are produced in Kerr media under conditions of anomalous group velocity dispersion (AGVD). Similar to diffraction in space, AGVD implements the WP phase–amplitude conversion in time due to phase modulation. Thus, the compression is implemented both in space and in time, forming a light bullet. For most transparent dielectrics, the anomalous dispersion of group velocity occurs in the mid-IR wavelength range. The studies of LBs are now extensively progressing due to the appearance of high-power optical parametric oscillators (OPO) in this range.

The possibility of LB formation during filamentation of femtosecond radiation in transparent dielectrics with AGVD was numerically studied in Ref. [3] based on the one-directional nonlinear wave equation in a dispersive medium, written in the spectral space for the light field. The formation of LBs and a sequence of LBs upon femtosecond filamentation were considered numerically in Ref. [4] in the slowly varying wave approximation [5]. For the first time the LB duration was measured in Refs [6, 7] during filamentation of pulsed radiation in fused silica at the wavelength 1800 nm. In the most compressed central region of the WP having a diameter of 50 μm, the LB duration amounted to about two optical oscillations at the carrier wavelength. The asymmetric temporal profile of the LB essentially differs from the Gaussian one and the ratio of the LB duration at the half-maximum level to the autocorrelation function width is equal to 0.44–0.5. The emergence of the second LB in the filament with increasing pulse energy was detected by the characteristic three-hump shape of the autocorrelation function. The evolution of the spatiotemporal intensity distribution in the LB was studied in Ref. [8] with the application of the elegant cross-correlation technique using the method [9] with a sharply wedged sample, whose displacement allows one to investigate the transformation of WP parameters and the LB formation with increasing distance along the filament, while the parameters of the input radiation remain unchanged. The structure of the LBs formed in sapphire during filamentation of pulsed radiation at the wavelength 1800 nm, reconstructed on the basis of these experiments, corresponds to a duration of 40 fs and a diameter of 15 μm. The structure comprises the central high-intensity core, surrounded by the region of low intensity with a Bessel-like pattern, which supports the energy localisation in the core in the process of propagation. The splitting of the second LB with increasing pulse energy was recorded in fused silica [10].

The LB formation is inseparably related to the generation of a broadband supercontinuum. The formation of each LB is accompanied by the 'ejection' of a discrete portion of anti-Stokes radiation in the visible range [11–13]. As a result, an isolated anti-Stokes supercontinuum wing is formed, the shift of which towards the short-wavelength region increases, and the spectral width decreases with increasing incident radiation wavelength [11, 14–18].

The current state of multiple studies of the broadband supercontinuum generation during filamentation of femtosecond laser radiation in transparent dielectrics is presented in review [19]. The study of LB and its spectrum regularities under AGVD filamentation conditions is an urgent problem of modern nonlinear femtosecond optics, the solution of which will allow the results of the laboratory and theoretical studies to be scaled to the up-to-date high-power mid-IR laser systems, in particular, the systems of atmospheric optics. In

E.D. Zaloznaya, A.E. Dormidonov, V.P. Kandidov Faculty of Physics, M.V. Lomonosov Moscow State University, Vorob'evy Gory, 119991 Moscow, Russia; International Laser Center, M.V. Lomonosov Moscow State University, Vorob'evy Gory, 119991 Moscow, Russia; **V.O. Kompanets, S.V. Chekalin** Institute for Spectroscopy, Russian Academy of Sciences, ul. Fizicheskaya 5, Troitsk, 108840 Moscow, Russia; e-mail: chekalin@isan.troitsk.ru

Received 16 February 2018
Kvantovaya Elektronika **48** (4) 366–371 (2018)
Translated by V.L. Derbov

order to solve this problem, a general equation for the LB spectrum was derived [20]. This equation determines the anti-Stokes shift of the isolated band of the LB supercontinuum in different media. The generality of the obtained dispersion equation is confirmed by the results of all known experimental studies performed in different condensed media, with femtosecond radiation at the wavelength fixed or tunable in the mid-IR range [15–18, 21–28]. The established regularity allows prediction of the anti-Stokes supercontinuum wing maximum position, radiated by the LB, for any dielectric with the known dispersion law.

The domain of LB existence in the space of variables that determine the WP energy and the dispersion of its group velocity in the medium was determined in Ref. [29] based on the analysis of the integrals of motion for the equation describing the slowly varying WP envelope in the medium with Kerr nonlinearity. The experimental studies of the effect of the group velocity dispersion parameter $|k_2|$ on the WP dynamics in fused silica and sapphire were carried out in Ref. [27] using the method of three-dimensional imaging. The temporal decay of the WP was recorded at the wavelength 1450 nm, at which in the considered media $|k_2| = 11$ fs^2 mm^{-1}, and the compression of WP at the wavelengths 1800 and 2250 nm, for which $|k_2| > 60$ fs^2 mm^{-1}. According to the theoretical studies of self-compression of soliton-like WPs in a nonlinear medium, performed in Ref. [30], the nonlinearity of material dispersion can suppress the instability of short pulses during filamentation. As shown in Ref. [31], at the peak WP power exceeding the critical power of stationary self-focusing, a sequence of LBs is formed if the dispersion and diffraction lengths are close, and only a single LB is generated if these lengths strongly differ from each other. Chekalin et al. [32] studied the effect of the ratio of dispersion to diffraction length on the formation of LB and supercontinuum in fused silica and fluorides during filamentation of pulsed radiation, whose peak power exceeds the critical power of stationary self-focusing by 1.5–2 times. It was found that if the dispersion length significantly exceeds the diffraction one, then the formation of LBs and the short-wavelength shift of the anti-Stokes wing in the supercontinuum depend on the pulse energy, while at close values of the characteristic lengths this dependence was not observed. The latter fact is an evidence of the coordinated WP compression in space and time in the process of LB formation.

In the present paper, we study the effect of the ratio of diffraction to dispersion length of a femtosecond WP on the threshold power of its filamentation and the formation of an LB during its propagation in solid-state dielectrics with anomalous group velocity dispersion.

2. Formulation of the problem

Filamentation is studied numerically within the approximation of a slowly varying wave that describes a WP with the duration close to the period of a single optical oscillation, propagating through a nonlinear dispersion medium [5]. In the coordinate system moving with the group velocity, the equation for the WP envelope $A(r,t,z)$ with the centre frequency ω_0 has the form [11]

$$2ik_0\frac{\partial A}{\partial z} = \hat{T}^{-1}\Delta_\perp A + \int_{-\infty}^{\infty}\frac{1}{1+\Omega/\omega_0}(k^2(\omega_0+\Omega) - (k_0+k_1\Omega)^2)\tilde{A}(r,\Omega,z)\exp(i\Omega t)\,d\Omega + \frac{2k_0^2}{n_0}\hat{T}[\Delta n_k A] + \frac{2k_0^2}{n_0}\hat{T}^{-1}[\Delta n_p A] - ik_0\hat{T}^{-2}[\sigma N_e A] - ik_0\alpha A. \quad (1)$$

Here, $\tilde{A}(r,\Omega,z)$ is the Fourier transform of the WP envelope; $\Omega = \omega - \omega_0$ is the frequency shift of the supercontinuum harmonic at the frequency ω from the carrier frequency ω_0; $k_0 = k(\omega_0)$; and $k(\omega) = \omega n(\omega)/c_0$, where $n(\omega)$ is the dispersion law for the material, described by the Sellmeier formula; c_0 is the velocity of light in vacuum; k_1^{-1} is the group velocity; Δn_k and Δn_p are the increments of the refractive index caused by Kerr and laser plasma nonlinearity, respectively; σ is the cross section of the inverse-bremsstrahlung absorption; N_e is the concentration of electrons; α is the attenuation coefficient for photoionisation; and $\hat{T} = 1 - (i/\omega_0)(\partial/\partial t)$ is the operator of wave nonstationarity. Equation (1) was considered together with the kinetic equation, in which the electron generation rate was determined using the Keldysh formula [33]. The system of equations obtained in this way describes the WP diffraction and dispersion, the effect of wave front self-steepening, the nonstationary changes in the medium refractive index, the attenuation of radiation caused by the bremsstrahlung absorption and the photoionisation losses.

The wave packet incident on the input face of the sample was taken to be a transform-limited pulse with the Gaussian distribution of the field amplitude in the cross-section plane and in time

$$A(r,t,z=0) = A_0\exp\left(-\frac{r^2}{2a_0^2} - \frac{\tau^2}{2\tau_0^2}\right), \quad (2)$$

where a_0 and τ_0 are the WP radius and half-duration at the e^{-1} intensity level; and A_0 is the peak amplitude of the light field.

To investigate the influence of the ratio of the diffraction length ($L_{dif} = ka_0^2$) to the dispersion length ($L_{disp} = \tau_0^2/|k_2|$, where $k_2 = \partial^2 k/\partial\omega^2$) of the input pulse on the filamentation and LB formation, we considered the propagation of femtosecond WPs in fused silica, CaF_2, and LiF at the wavelengths 2000, 3000, and 3100 nm, respectively. These wavelengths lie in the region of anomalous group velocity dispersion of these media. Since in the experiment the variation of the parameter L_{dif}/L_{disp} for the transform-limited radiation was implemented by changing the radius of the input beam a_0 during the replacement of the lens focusing the radiation onto the input face of the sample, we simulated numerically the propagation of WPs with variable energy and diffraction length L_{dif} and constant dispersion length L_{disp}.

At the wavelength 2000 nm the parameter τ_0 equals 30 fs, and in the fused silica with $k_{2SiO_2} = -100$ fs^2 mm^{-1} the dispersion length is $L_{disp} = 9$ mm. The increase in the beam radius from 10.5 to 160 μm corresponds to the variation of the diffraction length within 0.5–115 mm and of the ratio L_{dif}/L_{disp} within 0.12–13. At the wavelengths 3000 and 3100 nm $\tau_0 =$ 60 fs; in LiF and CaF_2 with the dispersion parameters $k_{2LiF} =$ –267 fs^2 mm^{-1}, $k_{2CaF_2} = -105$ fs^2 mm^{-1} at the considered wavelengths the corresponding dispersion lengths L_{disp} are equal to 13.5 and 34 mm. In the numerical simulations the variation of L_{dif} was performed in such a range that the ratio L_{dif}/L_{disp} varied in the same interval as for the fused silica.

As an example, Fig. 1 presents the spatiotemporal intensity distributions $\lg(I(r,t)/I_0)$ in the LB at a number of charac-

teristic distances from the medium input (I_0 is the peak intensity of the initial WP). The Figure demonstrates the evolution of the intensity distribution in the process of wave packet propagation in LiF at $L_{dif} = L_{disp}$ and the peak power $P = 1.2P_{cr}$, where $P_{cr} = 3.77\pi n_0/(2k_0^2 n_2)$ is the critical power of stationary self-focusing. Note that the spatiotemporal self-compression of the 3D WP is determined by its energy [30]. However, for the unchanged duration of the femtosecond radiation, implemented in the experiments with transform-limited pulses, the equivalent energy characteristic determining the nonlinear optical interaction with the medium is the peak power P, which is commonly used in practical estimates.

The distribution $\lg(I(r,t)/I_0)$ in Fig. 1a ($z = 0$) corresponds to the incident radiation, for which the lines of equal intensity have the shape of concentric circles. Figure 1b shows the emergence of a LB in the WP. Since in the considered case the dispersion length is close to the diffraction one ($L_{dif} \approx L_{disp}$), the wave packet compression in the cross section plane occurs in accordance with the temporal compression. The lines of equal intensity remain circular until the formation of the LB and the beginning of plasma generation, which manifests itself by a narrow diverging tail in the intensity distribution, caused by defocusing in the plasma. The appearance of plasma is a criterion of the formation of a high-intensity LB (Fig. 1b), and $z = 19.9$ mm can be considered as the distance at which the filamentation starts (L_{fil}). The character of further WP propagation is presented in Fig. 1c, where the region of high intensity is maximally compressed in time and stretched in the cross section plane, and in Fig. 1d, where the radius of the high-intensity region in the central part of the WP decreases, and the duration, on the contrary, increases. In the process of further WP propagation the intensity in the LB falls, and next bullets are not formed.

3. Threshold of WP filamentation and LB formation

Let us introduce the notion of the threshold power of femtosecond pulse filamentation (P_{th}) as the minimal power at which the LB is formed. Figure 2 presents the axial peak intensity $I_{peak}(r = 0, z)$ and concentration of electrons $N_e(r = 0, z)$ versus the propagation distance z, which reproduce the scenario of LB formation in LiF. The presented results are obtained by numerical simulation of femtosecond WP propagation at the wavelength 3100 nm with different peak powers. In the WP with the energy $W = 11.8$ μJ the axial intensity decreases with distance. With a minor increase in energy to $W = 12.8$ μJ, the intensity and the electron concentration dramatically increase at the distance $z = 19.9$ mm, which is an evidence of the filament and LB formation. The value of the peak power obtained in this way will be accepted as the threshold power P_{th} of filamentation and LB formation.

In the process of WP propagation with the power, equal to the threshold power of filamentation P_{th} in the dielectric under the conditions of AGVD, a single LB is formed characterised by the intensity increase to 140 TW cm^{-2} and detected by a sharp increase in the concentration of free electrons at the filament axis. If $P < P_{th}$, the LB is not formed, which is

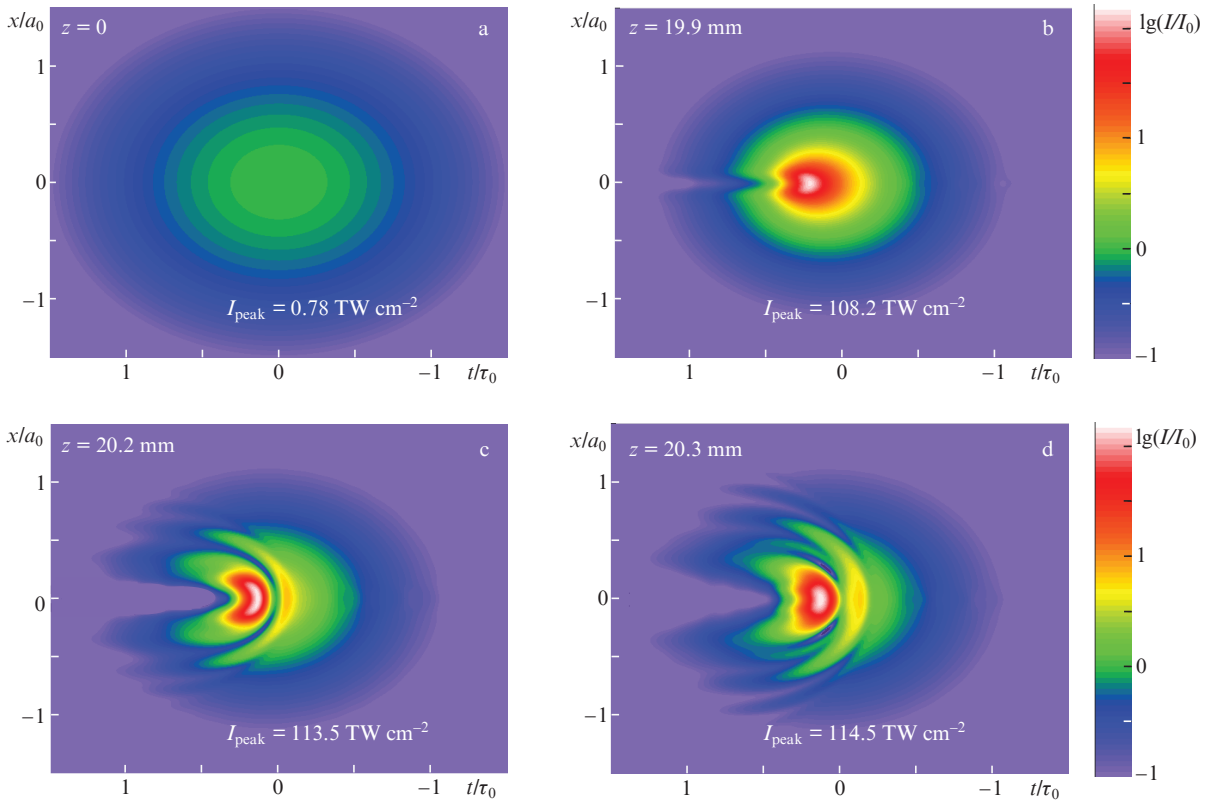

Figure 1. (Colour online) Spatiotemporal intensity distributions $I(r,t)$ presented in the logarithmic brightness scale $\lg(I(r,t)/I_0)$ for the wave packet with the peak energy 12.8 μJ at the wavelength 3100 nm in LiF at the characteristic distances z = (a) 0, (b) 19.9, (c) 20.2, and (d)20.3 mm.

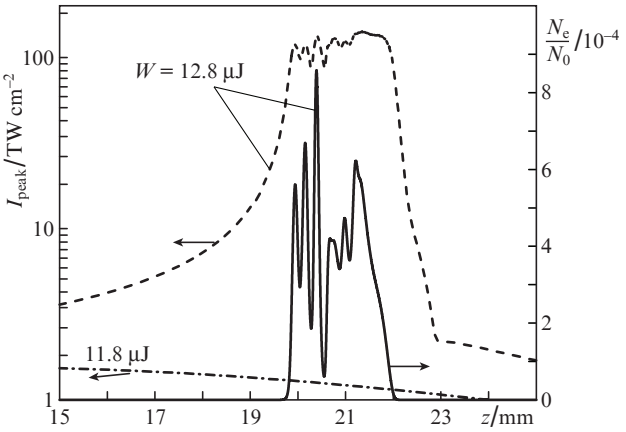

Figure 2. Peak intensity I_{peak} $(r = 0, z)$ and concentration of electrons $N_e(r = 0, z)$ vs. propagation length at the z axis during pulsed radiation filamentation at the wavelength 3100 nm in LiF at $W = 11.8$ ($P < P_{th}$) and 12.8 μJ ($P = P_{th}$).

seen from a decrease in the WP intensity and the absence of plasma (see Fig. 2).

The values of the threshold power of filamentation and LB formation as functions of L_{dif}/L_{disp} obtained for fused silica, LiF, and CaF_2 are presented in Fig. 3. It is seen that the values of the threshold power P_{th} scaled to the critical power of stationary self-focusing P_{cr} for WPs with different wavelengths in all considered dielectrics lie on one curve of the dependence on the ratio L_{dif}/L_{disp}. This fact means that the ratio L_{dif}/L_{disp} is a similarity parameter for the process of filamentation emergence and LB formation upon propagation of a mid-IR WP in a transparent dielectric with AGVD.

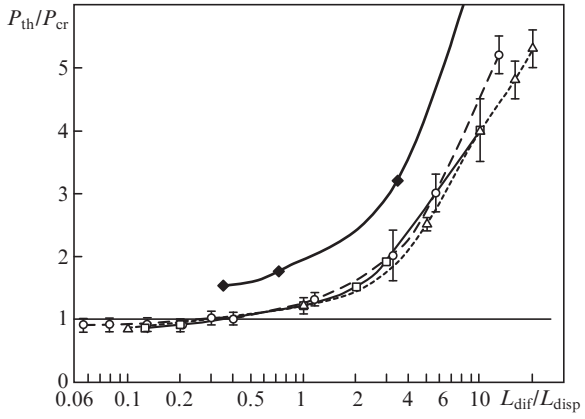

Figure 3. Threshold power of filamentation and LB formation scaled to the critical power of stationary self-focusing vs. the similarity parameter L_{dif}/L_{disp} [experiment, fused silica (♦); numerical modelling, fused silica (○), LiF (□), CaF_2 (△)].

The experimental studies of LB formation were carried out at the femtosecond complex based on a TOPAS tunable parametric amplifier, combined with a Spitfire Pro regenerative amplifier. The dependence of the threshold power P_{th}/P_{cr} of LB formation on the parameter L_{dif}/L_{disp} was obtained in fused silica with the pulses having the wavelength 1900 nm and the duration 50 fs at the half-maximum level. The output beam having the diameter 3.0–3.5 mm (at the half-maximum level) was focused onto the input face of the rectangular sample 15 cm long. To vary the diffraction length of the input radiation we used lenses with different focal lengths F. Thus, at $F = 1$ m the beam diameter at the input face of the sample amounted to 280 μm (at the half-maximum level) and the diffraction length was $L_{dif} = 158$ mm; for $F = 0.585$ m $L_{dif} = 44$ mm, and for $F = 0.295$ m $L_{dif} = 9$ mm. To determine the LB formation threshold, the pulse energy was increased until the appearance of characteristic glow of the SC anti-Stokes wing scattered in the sample, which was recorded using a photo camera through the side face of the sample with a 10 s exposure. As an example, Fig. 4 presents the pulse tracks, recorded at different radiation energies, having the diameter 135 μm at the input face of the sample under focusing with $F = 0.585$ m. The scattered radiation of the supercontinuum appears at the energy 2.95 μJ, which corresponds to the peak power 53 MW, equal to the threshold P_{th} for the formation of LB in fused silica.

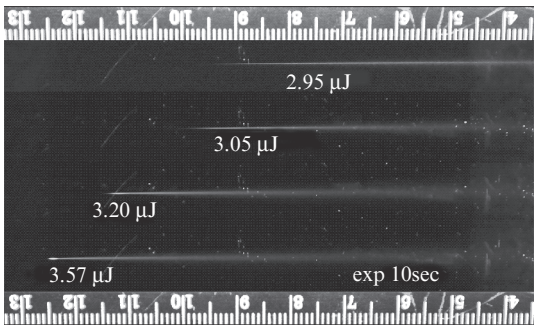

Figure 4. Experimental images of the supercontinuum radiation scattered in the sample and the glow of plasma generated in fused silica during filamentation of a pulse at the wavelength 1900 nm with the duration 50 fs (at half-maximum level) for the increasing pulse energy.

The dependence of the relative threshold power P_{th}/P_{cr} on the parameter L_{dif}/L_{disp}, based on the experimental results (Fig. 3), is similar to the curve calculated numerically. The systematic deviation of the experimental values of the threshold power from the calculated ones is due to the linear losses in the sample that grow with distance from the input to the filamentation onset with increasing diffraction length. Thus, at $L_{dif}/L_{disp} = 16$ the measured threshold power is $P_{th} = 8.6P_{cr}$, while the calculated value is $P_{th} = 4.8P_{cr}$.

4. Analysis of the results

For physical interpretation of the obtained dependence of the threshold power P_{th}/P_{cr} on the similarity parameter L_{dif}/L_{disp}, let us consider the evolution of the spatiotemporal intensity distribution in the WP. At $L_{dif}/L_{disp} \gg 1$ the self-focusing of the WP in space lags behind its transformation in time. In this case, at the initial stage of propagation before the appearance of nonlinear effects the strong spreading of the WP in time occurs due to the dispersion, which decreases its peak intensity (Fig. 5a). The initiation of a LB is still possible if the intensity and, therefore, nonlinear phase modulation of the light field is large enough for the WP compression in space and time (Fig. 5a). Since the peak intensity of WP significantly decreases at the beginning of propagation due to the dispersion, the threshold power P_{th} of the pulse necessary for the filament formation appears to be significantly higher than the critical power of stationary self-focusing P_{cr}. Thus,

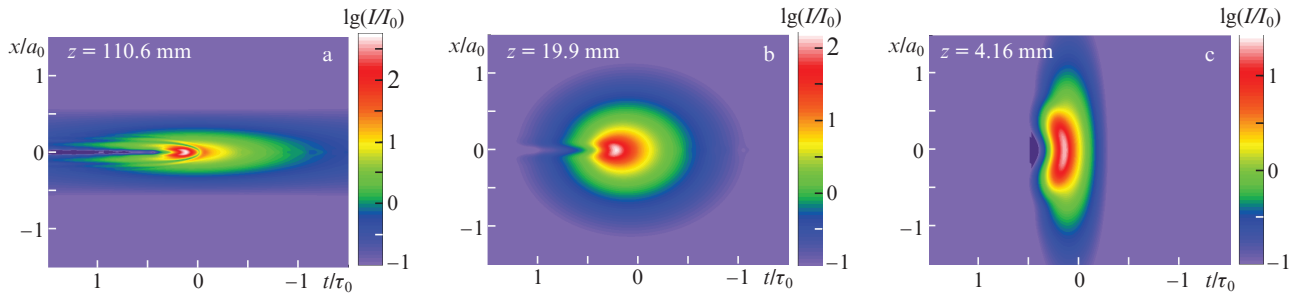

Figure 5. (Colour online) Spatiotemporal intensity distributions $I(r,t)$ in the wave packet, presented in logarithmic brightness scale $\lg(I(r,t)/I_0)$ at the characteristic distances in LiF at (a) similarity parameter $L_{dif}/L_{disp} = 10$ and the peak power $P_0 = P_{th} = 4P_{cr}$, (b) $L_{dif}/L_{disp} = 1$ and $P_0 = P_{th} = 1.2P_{cr}$, and (c) $L_{dif}/L_{disp} = 0.1$, $P_0 = P_{th} = 0.85P_{cr}$.

in a WP with the parameter $L_{dif}/L_{disp} = 10$ the filament and LB are formed in LiF at the threshold power $P_{th} = 4P_{cr}$, with $L_{dif}/L_{disp} = 13$ in the fused silica at $P_{th} = 5.2P_{cr}$, and with $L_{dif}/L_{disp} = 20$ in CaF_2 at $P_{th} = 5.3P_{cr}$ (see Fig. 3).

The observed growth of the filamentation threshold at the increasing ratio of the WP diffraction length to the dispersion one confirms the analytical estimates obtained in Ref. [30] for the WP whose longitudinal size is much smaller than the transverse one. According to this paper, the self-focusing threshold of such WPs at the adiabatic reduction of its duration depends on the transverse size and increases proportionally to the square of its width.

At $L_{dif}/L_{disp} \approx 1$ the WP compression in space and in time occurs simultaneously, so that the intensity distribution $I(r,t)$ remains similar to the initial one till the formation of the LB with high intensity and the appearance of defocusing in the laser-induced plasma (Fig. 5b). In this case, the lines of equal intensity in the WP remain circular until the plasma generation. At the coordinated self-compression of radiation in space and time the threshold power P_{th} insignificantly exceeds the critical power of stationary self-focusing P_{cr}. Thus, in LiF and CaF_2 at $L_{dif}/L_{disp} = 1$ the threshold power of filamentation is $P_{th} = 1.2P_{cr}$ (see Fig. 3). This excess is related to the effect of higher-order dispersion that distorts the pulse shape.

If $L_{dif}/L_{disp} \ll 1$, then the distance at which the dispersion effects manifest themselves is large, and the spatial compression of WPs is close to stationary one, for which it was expected that $P_{th} = P_{cr}$. However, it appeared that the threshold power P_{th} of the femtosecond WP filamentation and LB formation is smaller than the critical power of stationary self-focusing P_{cr} (see Fig. 3). In this case at the peak power $P_{th} < P_{cr}$ the temporal compression of WP due to the self-phase modulation in a Kerr medium increases with distance because of the formation of a narrow peak under predominating spatial compression in the central temporal layers. As a result, the WP compression in space and time becomes coupled, which leads to the reduction of the threshold power of femtosecond WP filamentation and LB formation under AGVD conditions. Upon further propagation the pulse intensity in the near-axis region increases and the LB is formed (Fig. 5c) For all the three media considered at $L_{dif}/L_{disp} \approx 0.1$ the threshold power of filamentation P_{th} amounts to $(0.85-0.9)P_{cr}$.

5. Conclusions

The ratio of the WP diffraction length to its dispersion length L_{dif}/L_{disp} is a similarity parameter that determines the process of filamentation and light bullet formation under the nonlinear optical interaction of a high-power mid-IR femtosecond laser pulse with transparent dielectrics under the conditions of anomalous group velocity dispersion. The threshold power P_{th} of the filament and LB formation in the wave packet propagating through different dielectrics, scaled to the critical power of stationary self-focusing P_{cr}, does not depend on the radiation wavelength and the nonlinear dispersion medium parameters and is determined by the similarity parameter L_{dif}/L_{disp}. The change in the relative threshold power P_{th}/P_{cr} of filamentation and LB formation in transparent dielectrics obeys the unique dependence on the introduced similarity parameter. The threshold power P_{th}/P_{cr} steadily increases with increasing parameter L_{dif}/L_{disp} in the region of its values greater than unity. The excess of P_{th} over P_{cr} at $L_{dif}/L_{disp} > 1$ is caused by the dispersion spreading of the WP at the beginning of propagation before the emergence of nonlinear effects, which leads to the peak power reduction and, therefore, to an increase in the threshold power of filamentation. Thus, at $L_{dif}/L_{disp} = 10$ the threshold power $P_{th} > 4P_{cr}$. For the similarity parameter $L_{dif}/L_{disp} \approx 1$ the coordinated compression of WPs in both space and time occurs, for which $P_{th} \approx 1.2P_{cr}$. This is due to the pulse shape distortion by the higher-order dispersion effects. At $L_{dif}/L_{disp} \ll 1$ the filamentation threshold power is smaller than the critical power of self-focusing [$P_{th} = (0.85-0.9)P_{cr}$], which is related to the growth of intensity at self-focusing and the formation of a narrow peak in the centre of WP, the duration of which is smaller than that of the incident pulse.

Acknowledgements. The work was supported by the Presidium of the Russian Academy of Sciences (Programme 'Extreme Light Fields and Their Interaction with Matter) and the Russian Foundation for Basic Research (Grant No. 18-02-00624). The experiments were performed using the unique research setup 'Multipurpose Femtosecond Laser Diagnostic Spectrometric Complex' at the Institute of Spectroscopy of RAS.

References

1. Silberberg Y. *Opt. Lett.*, **15**, 1282 (1990).
2. Akhmanov S.A., Vysloukh V.A., Chirkin A.S. *Optics of Femtosecond Laser Pulses* (New York: American Institute of Physics, 1992; Moscow: Nauka, 1988).
3. Berge L., Skupin S. *Phys. Rev. Lett.*, **100**, 113902 (2008).
4. Smetanina E.O., Dormidonov A.E., Kandidov V.P. *Laser Phys.*, **22**, 1189 (2012).
5. Brabec T., Krausz F. *Phys. Rev. Lett.*, **78**, 3282 (1997).

6. Smetanina E.O., Kompanets V.O., Dormidonov A.E., Chekalin S.V., Kandidov V.P. *Laser Phys. Lett*., **10**, 10540 (2013).
7. Chekalin S.V., Kompanets V.O., Smetanina E.O., Kandidov V.P. *Quantum Electron*., **43**, 326 (2013) [*Kvantovaya Elektron*., **43**, 326 (2013)].
8. Majus D., Tamošauskas G., Gražulevičiūtė I., Garejev N., Lotti A., Couairon A., Dubietis A. *Phys. Rev. Lett*., **112**, 193901 (2014).
9. Kandidov V.P., Smetanina E.O., Dormidonov A.E., Kompanets V.O., Chekalin S.V. *JETP*, **113**, 422 (2011) [*Zh. Eksp. Teor. Fiz*., **140**, 484 (2011)].
10. Gražulevičiūtė I., Šuminas R., Tamošauskas G., Couairon A., Dubietis A. *Opt. Lett*., **40**, 3719 (2015).
11. Smetanina E.O., Kompanets V.O., Chekalin S.V., Kandidov V.P. *Quantum Electron*., **42**, 913 (2012) [*Kvantovaya Elektron*., **42**, 913 (2012)].
12. Chekalin S.V., Kompanets V.O., Dokukina A.E., Dormidonov A.E., Smetanina E.O., Kandidov V.P. *Quantum Electron*., **45**, 401 (2015) [*Kvantovaya Elektron*., **45**, 401 (2015)].
13. Chekalin S.V., Dokukina A.E., Dormidonov A.E., Kompanets V.O., Smetanina E.O., Kandidov V.P. *J. Phys. B: Atomic, Molec. Opt. Phys*., **48**, 094008 (2015).
14. Smetanina E.O., Kompanets V.O., Chekalin S.V., Kandidov V.P. *Quantum Electron*., **42**, 920 (2012) [*Kvantovaya Elektron*., **42**, 920 (2012)].
15. Smetanina E.O., Kompanets V.O., Chekalin S.V., Dormidonov A.E., Kandidov V.P. *Opt. Lett*., **38**, 16 (2013).
16. Durand M., Lim K., Jukna V., McKee E., Baudelet M., Houard A., Richardson M., Mysyrowicz A., Couairon A. *Phys. Rev. A*, **87**, 043820 (2013).
17. Vasa P., Dharmadhikari J.A., Dharmadhikari A.K., Sharma R., Singh M., Mathur D. *Phys. Rev. A*, **89**, 043834 (2014).
18. Dormidonov A.E., Kompanets V.O., Chekalin S.V., Kandidov V.P. *Opt. Express*, **23**, 29202 (2015).
19. Dubietis A., Tamošauskas G., Šuminas R., Jukna V., Couairon A. *Lithuanian J. Phys*., **57**, 113 (2017).
20. Dormidonov A.E., Kompanets V.O., Chekalin S.V., Kandidov V.P. *JETP Lett*., **104**, 175 (2016) [*Pis'ma Zh. Eksp. Teor. Fiz*., **104**, 173 (2016)].
21. Saliminia A., Chin S.L., Vallée R. *Opt. Express*, **13**, 5731 (2005).
22. Naudeau M.L., Law R.J., Luk T.S., Nelson T.R., Cameron S.M., Rudd J.V. *Opt. Express*, **14**, 6194 (2006).
23. Silva F., Austin D.R., Thai A., Baudisch M., Hemmer M., Faccio D., Couairon A., Biegert J. *Nat. Commun*., **3**, 807 (2012).
24. Darginavičius J., Majus D., Jukna V., Garejev N., Valiulis G., Couairon A., Dubietis A. *Opt. Express*, **21**, 25210 (2013).
25. Dharmadhikari J.A., Deshpande R.A., Nath A., Dota K., Mathur D., Dharmadhikari A.K. *Appl. Phys. B*, **117**, 471 (2014).
26. Liang H., Krogen P., Grynko R., Novak O., Chun-Lin Chang, Gregory J., Stein Gr.J., et al. *Opt. Lett*., **40**, 1069 (2015).
27. Gražulevičiūtė I., Garejev N., Majus D., Jukna V., Tamošauskas G., Dubietis A. *J. Opt*., **18**, 0255022016 (2016).
28. Garejev N., Tamošauskas G., Dubietis A. *J. Opt. Soc. Am. B*, **34**, 88 (2017).
29. Bergé L., Skupin S. *Phys. Rev. E*, **71**, 065601 (2005).
30. Balakin A.A., Litvak A.G., Mironov V.A., Skobelev S.A. *J. Opt*., **19**, 095503 (2017).
31. Zaloznaya E.D., Dormidonov A.E., Kandidov V.P. *Opt. Atmos. Okeana*, **29**, 184 (2016).
32. Chekalin S.V., Kompanets V.O., Dormidonov A.E., Zaloznaya E.D., Kandidov V.P. *Quantum Electron*., **47**, 252 (2017) [*Kvantovaya Elektron*., **47**, 252 (2017)].
33. Keldysh L.V. *JETP*, **20** (5), 1307 (1965) [*Zh. Eksp. Teor. Fiz*., **47**, 1945 (1965)].